

# Electronic Structure and Magnetic Properties of $\text{-Ti}_5\text{Sn}_5$

T. Jeong

Department of Physics, University of California, Davis, California 95616

The electronic structure of  $\text{-Ti}_5\text{Sn}_5$  has been studied based on the density functional theory within the local-density approximation. The calculation indicates that  $\text{-Ti}_5\text{Sn}_5$  is very close to ferromagnetic instability and shows ferromagnetic ordering after rare earth element doping. Large enhancement of the static susceptibility over its non-interacting value is found due to a peak in the density of states at the Fermi level.

PACS numbers: 71.28.+d, 75.10.Lp, 71.18.+y, 71.20.Lp

## I. INTRODUCTION

Electronic systems close to magnetic instability has drawn a lot of both experimental and theoretical attention because of their interesting and often unexpected properties arising from the interaction of electrons with the magnetic fluctuations. Recently close-to-ferromagnetic behavior was observed in  $\text{-Ti}_5\text{Sn}_5$  [1]. This compound shows a very interesting unusual magnetic characteristics. Especially magnetic and specific heat measurements indicate that this compound is very close to ferromagnetic instability and shows ferromagnetic ordering after rare earth element doping. This compound joins other prototype itinerant ferromagnets  $\text{ZrZn}_2$ ,  $\text{Sc}_3\text{In}$  and  $\text{TiBe}_{2-x}\text{Cu}_x$ . Resistivity and magnetic susceptibility measurements of this compound show the Pauli paramagnet displaying Fermi liquid behavior, an indication that the Ti is in the  $4^+$  and not the magnetic  $3^+$  state. The value of  $\chi_0$  from the susceptibility measurements is  $1.1 \times 10^{-6} \text{ emu/g}$ , which is typical value of intermetallic compounds. An interesting result comes from the heat capacity measurement. The heat capacity was measured in the temperature range 350mK  $\leq T \leq$  25K and straight line which fits to the low temperature part of the  $\frac{C}{T}$  versus  $T^2$  gives a value of  $(\chi_0) = 40 \text{ mJ/K}^2 \text{ mol}$ . Using the values of  $\chi_0 = 1.1 \times 10^{-6} \text{ emu/g}$  and  $\chi_0$ , Dymitov and coworkers estimated the Wilson ratio  $R_W = 1.76$  which indicates that  $\text{-Ti}_5\text{Sn}_5$  is a correlated system [1]. Another interesting results are the effects of doping with rare earth elements. The small amounts of Ce, La or Co impurities drove the system to the ferromagnetic (FM) state, with the ordering temperatures of the order of 150 K. It was shown that the magnetic behavior is intrinsic to the  $\text{-Ti}_5\text{Sn}_5$ , i.e., it is not the case of magnetic impurities in non-magnetic host. For example, the susceptibility measurements on  $\text{La}_x\text{-Ti}_5\text{Sn}_5$  show ferromagnetic ordering with a critical temperature equal to  $T_c = 160 \text{ K}$ . The constituent elements are non-magnetic, with the exception of Ti which in the  $\text{Ti}^{4+}$  configuration carries an effective moment of  $1.8 \mu_B$ . Susceptibility measurements of the undoped  $\text{-Ti}_5\text{Sn}_5$  show the Pauli paramagnetism, which is an indication that the Ti is in a non-magnetic ground state.

In this paper we investigate the electronic and magnetic properties of  $\text{-Ti}_5\text{Sn}_5$  based on density functional

theory. In particular we have calculated the bandstructures, Fermi surfaces and linear specific heat coefficient. Large enhancement of the static susceptibility over its non-interacting value is found due to a peak in the density of states at the Fermi level.

## II. CRYSTAL STRUCTURE

The crystal structure of  $\text{-Ti}_5\text{Sn}_6$  belongs to the non-symorphic hexagonal space group  $P6_3/mmc$ . This crystal structure is described in detail by Kleinknecht [2]. There are three distinct Sn sites,  $((0,0,0), (1/3,2/3,1/4), (0.795, 0.590, 1/4))$  with site symmetries  $6m2$ ,  $6m2$  and  $mm2$  respectively and two Ti sites  $((1/2, 0, 0), (0.165, 0.330, 1/4))$  with site symmetries  $2m$  and  $mm2$  respectively. It does not seem to be a simple manner in which to see the structure but it appears that the Ti sites form groups of tetrahedral along the (001) direction.  $\text{-Ti}_5\text{Sn}_6$  is the only known compound which forms this structure. The lattice constants  $a$  and  $c$  are 9.24 Å and 5.71 Å respectively. There are two formula units per primitive cell.

Alternatively the crystal structure of  $\text{-Ti}_5\text{Sn}_6$  can be viewed as ABAB'A stacking of Ti and Ti-Sn layers with a separation of  $c=4$ . The A-plane contains 3 Ti atoms per unit cell forming a 2D Kagome lattice. The B-plane contains 3 Ti and 5 Sn atoms. It is interesting to note that Ti atoms in the B-plane form slightly distorted Kagome lattice (the deviations from the ideal bond length being 1%). The B'-layer is the inversion image of the B-layer. The in-plane nearest-neighbor Ti-Ti distances are 4.61 Å (A-plane) and 4.61  $\pm$  0.05 Å (B-plane).

## III. METHOD OF CALCULATIONS

We have calculated the electronic structure using the full-potential nonorthogonal local-orbital minimum-basis (FPLO) method [3] to solve the Kohn-Sham equations of density functional theory. Scalar relativistic approximation and the exchange-correlation functional of Perdew and Wang [4] were used throughout this work. Ti  $3s; 3p; 4s; 4p; 3d$  states and Sn  $4s; 4p; 5s; 5p; 4d$  were included as valence states. All lower states were treated as core states. We included the relatively extended semi-

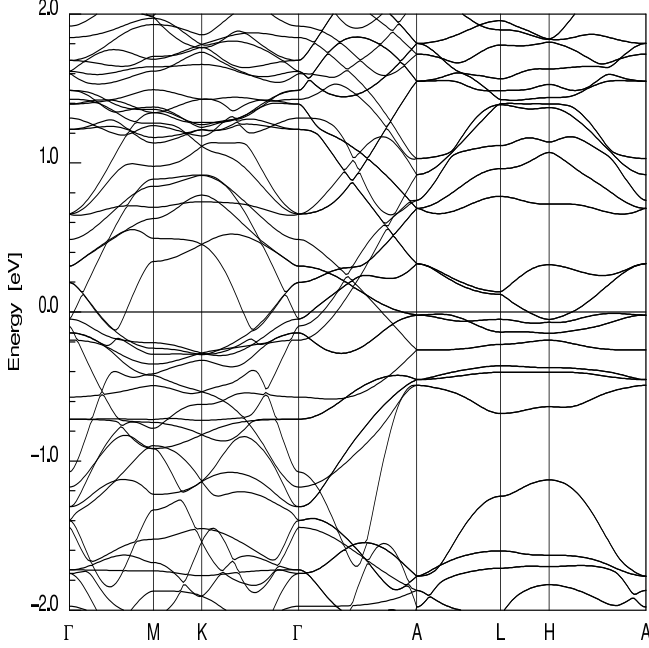


FIG. 1: The LDA bandstructure of non-magnetic  $\text{TiSn}_5$  along symmetry lines showing that there are several bands with weak dispersion being of primarily Ti 3d character near the Fermi level.

core 3s, 3p states of Ti and 4s, 4p, states of Sn as band states because of the considerable overlap of these states on nearest neighbors. This overlap would be otherwise neglected in our FPLO scheme. Ti 4p states were added to increase the quality of the basis set. The spatial extension of the basis orbitals, controlled by a conning potential ( $r=r_0$ )<sup>4</sup>, was optimized to minimize the total energy. The self-consistent potentials were carried out on a k mesh of 12 k points in each direction of the Brillouin zone, which corresponds to 133 k points in the irreducible zone. A careful sampling of the Brillouin zone is necessitated by the fine structures in the density of states near Fermi level  $E_F$ .

#### IV. RESULTS AND DISCUSSION

In Fig. 1 and Fig. 2 we show the bandstructure and the density of state respectively. The bands in the vicinity of the Fermi level have dominant Ti 3d character with the role of Sn to be merely to provide electrons. The Sn 5s bands lie between -10 eV and -5 eV. Around -5 eV there are Ti 4s states, above them the bands of Sn 5p spread over to the Fermi level. The Ti 3d bands lie between -2.5 eV and 5 eV and they dominate the Fermi level.

The bandstructure provides explanation of the rather high peaks in the density of state, in particular close to the Fermi level. While the bands in MK plane exhibit sizable dispersion their counterparts in the ALH plane are rather flat. We offer the following explanation of this

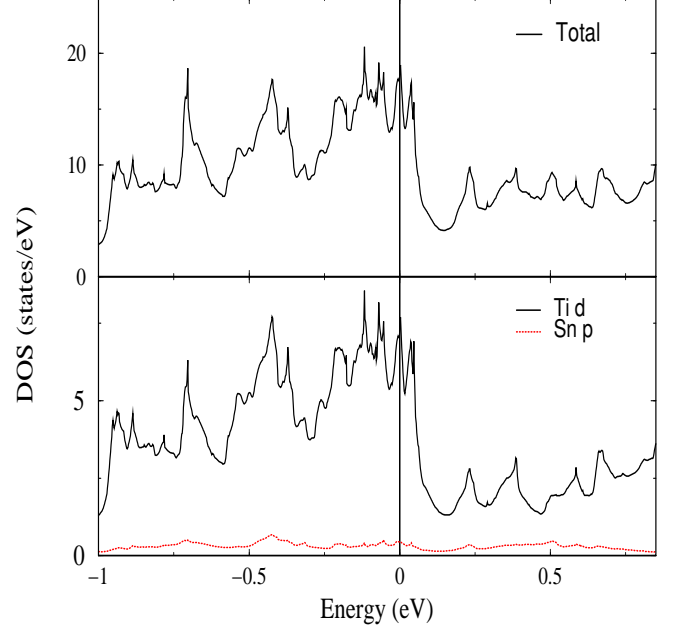


FIG. 2: Projected density of states of  $\text{TiSn}_5$ . Top panel: total density of states. Bottom panel: projection of the Ti 3d and Sn 5p, showing that Ti 3d character dominates the states near the Fermi level.

interesting feature. The Ti sublattice consists of Kagomé lattices, well known for a dispersionless band in their spectrum, coupled along the c-axis. Since the Ti-Ti inter-layer (A-A) bond is shorter than the Ti-Ti intra-layer distance, the inter-layer coupling is strong (see also A dispersion) and the bandstructure does not exhibit 2D features. However, the nearest neighbor inter-layer hopping does not contribute to the dispersion in the ALH plane. This can be shown by taking the  $k_z = \pi$  Bloch sums of the relevant d orbitals and considering the even parity of the d functions. Thus with the contribution of the main hopping being zero the ALH dispersion reflects the intra-layer hopping. The corresponding Fermi surfaces (FS) of  $\text{TiSn}_5$  is shown in Fig. ???. The point is located at the center of the hexagonal prism. The large FS in the middle panel of Fig. ??? is due to the Ti 3d states; the contribution of Sn states to these sheets is very small. We also calculated the LSDA magnetic band structures for the  $\text{TiSn}_5$ , in which the exchange splitting is almost negligible. Dymitris et al. [1] measured the linear specific heat coefficient for  $\text{TiSn}_5$  of  $\gamma = 40 \text{ mJ/K}^2 \text{ mole (formular unit)}$ . The calculated value of  $N(E_F) = 41.5 \text{ states/Ry/Ti}$  for  $\text{TiSn}_5$  corresponds to a bare value  $\gamma_b = 42.7 \text{ mJ/K}^2 \text{ mole (formular unit)}$ , which is in good agreement with the experimental one.

The presence of an electronic instability is signaled by a divergence of the corresponding susceptibility. In the

following we study the uniform magnetic susceptibility using the method of Janak [5]. The uniform magnetic susceptibility of a metal can be written as

$$\chi = \frac{\chi_0}{1 - N(E_F)I}; \quad (1)$$

where the numerator stands for the Pauli susceptibility of a gas of non-interacting electrons proportional to the density of states at the Fermi level  $N(E_F)$ , and the denominator represents the enhancement due to electron-electron interaction. Within the Kohn-Sham formalism of density functional theory the Stoner parameter  $I$  is related to the second derivative of the exchange-correlation functional with respect to the magnetization density. We have evaluated, within the density functional theory formalism, the Stoner enhancement of the susceptibility  $\chi = \frac{\chi_0}{1 - N(E_F)I}$ , where  $\chi_0 = 2 \frac{1}{N(E_F)}$  is the non-interacting susceptibility and  $S$  gives the electron-electron enhancement in terms of the Stoner constant  $I$ . We have calculated  $I$  using both the Janak-Vosko-Perdew theory [5] and fixed spin moment calculations [6]. The calculated density of states and Stoner parameter normalized per Ti atom are  $N(E_F) = 41.5$  states/Ry/Ti and  $I = 22.9$  mRy. By comparing the calculated value of the density of states with the measured susceptibility, a Stoner enhancement  $S = [1 - N(E_F)I]^{-1} = 20$  was obtained, indicating  $\text{-Ti}_2\text{Sn}_5$  a strongly exchange-enhanced metal. The presence of a peak close below the Fermi level suggest that a very small hole or electron doping can drive system into ferromagnetic regime.

The experimental reports [1] show that  $\text{-Ti}_2\text{Sn}_5$  is located at the boundary between non-magnetic and ferromagnetic ground state. This is supported by the large value of  $\chi$ , obtained from heat capacity measurements which corresponds to the peak at the density of states at the Fermi level. The transition to the ferromagnetic ground state occurs after a small amount of doping on the Ti site. Our fixed moment calculations clearly show that the  $\text{-Ti}_2\text{Sn}_5$  is located at the magnetic instability, which agrees very well with the experimental results. Itinerant magnetism is a consequence of an enhanced density of states at the Fermi level, consistent with the large values of  $\chi$  in the low temperature specific heat data and the magnetic moment is carried by the carriers that take part in the transport. The enhanced density of states and increase in electronic correlations produce the formation of a local moment whose magnitude is related to the band structure at the Fermi level.

## V. SUMMARY

Our fixed moment calculations clearly show that the  $\text{-Ti}_2\text{Sn}_5$  is located at the magnetic instability, which agrees very well with the experimental results. The calculation indicates that  $\text{-Ti}_2\text{Sn}_5$  is very close to ferromagnetic instability and shows ferromagnetic ordering after rare earth element doping. Large enhancement of the static susceptibility over its non-interacting value is found due to a peak in the density of states at the Fermi level.

- 
- [1] F. Dymiotis, J.C. Lashley, Z. Fisk, E. Peterson and S. Nakatsuji, *Philosophical Magazine* 83, No. 27, 3169 (2003).
  - [2] H. Kleinke, *J. Solid State Chem.* 159, 134 (2001).
  - [3] K. Koepf, and H. Eschrig, *Phys. Rev. B* 59, 1743 (1999); H. Eschrig, *Optimized LCAO Method and the electronic Structure of Extended Systems* (Springer, Berlin, 1989).
  - [4] J. P. Perdew, and Y. Wang, *Phys. Rev. B* 45, 13244 (1992).
  - [5] J. F. Janak, *Phys. Rev. B* 16, 255 (1977); S. H. Vosko

- and J. P. Perdew, *Can. J. Phys.* 53, 1385 (1975)
- [6] K. Schwarz and P. Mohn, *J. Phys. F* 14, L129 (1984)
- [7] T. Mori and A. Kawabata, *J. Phys. Soc. Japan* 34, 639 (1973); 35, 669 (1973)
- [8] D. L. Mills and P. Lederer, *J. Phys. Chem. Solids* 27, 1805 (1966)
- [9] J. Mathon, *Proc. Roy. Soc. A* 306, 355 (1968)
- [10] K. Ueda and T. Mori, *J. Phys. Soc. Japan* 39, 605 (1975)